CMS Physics Analysis Summary

Contact: cms-pag-conveners-b2g@cern.ch 2016/07/30

Search for singly-produced vector-like quarks decaying into a W boson and a bottom quark using the single lepton final state

The CMS Collaboration

Abstract

We present a search for the single production of a heavy vector-like quark, decaying into a W boson and a b quark. The search is performed using the data sample of pp collisions at a center of mass energy of $\sqrt{s} = 13$ TeV collected by the CMS experiment at the Large Hadron Collider in 2015. The dataset used in the analysis corresponds to 2.3 fb^{-1} of integrated luminosity. The search is carried out using events containing one electron or muon, at least one b-tagged jet with large transverse momentum, at least one jet in the forward region of the detector, and missing transverse energy. No excess over the standard model predictions is observed. Upper bounds are placed on the production cross section of heavy top quark partners, T quark with a charge of 2/3e and Y quark with a charge of $-4/3$e. The results are also interpreted as limits on the mass of the vector-like quark and its coupling to the W boson and the b quark. T quarks with masses below 1.73 TeV are excluded at 95% C.L. assuming a unit coupling and a BR(T$\rightarrow$Wb) = 0.5, while the expected limit is 1.42 TeV. Y quarks with coupling of 0.5 and BR(Y$\rightarrow$Wb) = 1 are excluded below 1.40 TeV, whereas the expected limit is 0.99 TeV.

1 Introduction

The standard model (SM) of particle physics has been exceptionally successful in describing the experimental phenomena at the subatomic scale. The observation of the Higgs boson with a mass of 125 GeV and with properties consistent with the SM expectations [1, 2] was the last missing piece for the confirmation of the SM. However, the SM cannot explain the Higgs mass value and requires large fine-tuning to accommodate it. New physics is warranted to stabilize the Higgs mass from the quantum corrections at the electroweak scale.

Many models beyond the SM have been proposed over the last several decades to resolve the fine-tuning problem. Some of the models postulate the existence of vector-like quarks (VLQ) [3–5], which are colored fermions with left- and right-chiral states, with both chiral states transforming in the same way under the $\mathrm{SU_C}(3) \times \mathrm{SU_L}(2) \times \mathrm{U_Y}(1)$ group. VLQ particles don't acquire masses through the Yukawa coupling to the Higgs boson and can play the role of the top partner to cancel the loop correction effects from the SM top quark to the Higgs boson mass.

Searches for VLQs have been already performed exploiting various decay modes. These searches were primarily focused on the pair production mechanism and they rule out VLQs with masses up to approximately 900 GeV [6–9]. The single VLQ production cross section is coupling-dependent, and at higher masses it can become the dominant production mechanism.

In this analysis, we present a search for single production of a heavy particle, that decays into a W boson and a b quark. This signature can arise from either a Y or a T quark with a charge of $-4/3$e and $2/3$e, respectively, produced in association with a light flavor quark and a b quark. The Feynman diagram for the Y and T quark production is shown in Figure 1. The outgoing light flavor quark in the upper part of the diagram produces a jet in the forward region of the detector, and it serves as a distinct characteristic of the single production in the event selection.

Within the VLQ phenomenology [10] the Y quark decays 100% into a b quark and a W boson, while the T quark may experience flavor-changing neutral current decays into tH and tZ. In the high-mass limit, the singlet T quark is expected to decay into bW 50% of the time.

The single VLQ production searches with Run II data were performed by CMS for T quark decaying into Ht and Zt. Upper limits on the production cross section times branching ratio are derived in the mass range of 700 GeV to 1800 GeV [11, 12].

The ATLAS collaboration published a search for single production of Y and T quarks decaying into bW using 8 TeV pp-collisions [13]. The analysis presented here is the first search using 13 TeV pp data, and sets the most stringent limits to-date on the single production cross section for these quarks. The search is performed using events with only one lepton (electron or muon), at least one b-tagged jet, at least one forward jet and a substantial missing transverse energy due to the escaping neutrino.

2 CMS Detector and event samples

The essential feature of the CMS detector is the superconducting solenoid, 6 m in diameter and 13 m in length, which provides an axial magnetic field of 3.8 T. Within the solenoid volume a multi-layered silicon pixel and strip tracker is used to measure the trajectories of charged particles with pseudorapidity $|\eta| < 2.5$. Outside of the tracker system electromagnetic calorimeter (ECAL) made of lead tungstate crystals and a hadronic calorimeter (HCAL) made of brass and scintillators cover a region $|\eta| < 3.0$. The region of $3.0 < |\eta| < 5.0$ is instrumented with steel

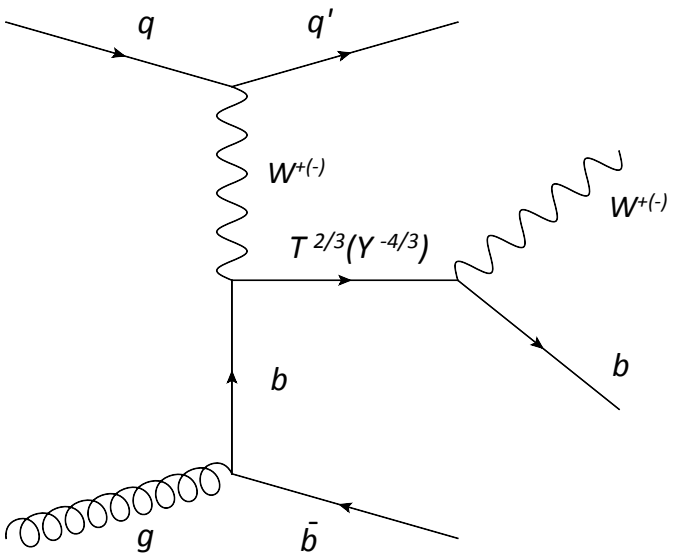

Figure 1: Leading order Feynman diagram for singly produced Y and T quarks.

and quartz fiber forward calorimeters. Muons are measured with gas detectors embedded in the return yoke outside of the solenoid and covering the region $|\eta| < 2.4$. The CMS detector is nearly hermetic, allowing for momentum balance measurements in the plane transverse to the beam direction. A detailed description of the CMS detector can be found elsewhere [14].

The data used for this analysis were recorded during the 2015 data taking period in proton-proton collisions at a center of mass energy of 13 TeV. The total integrated luminosity is 2.3 fb^{-1} collected with magnetic field of 3.8 T. The muon data sample was collected using a trigger based on presence of at least one isolated muon with $|\eta| < 2.1$ and $p_T > 20$ GeV. The electron data sample consists of events passing a single isolated electron trigger with $|\eta| < 2.5$ and $p_T > 27$ GeV.

Monte Carlo (MC) simulated samples are used to estimate signal efficiencies and background contributions. The $t\bar{t}$+jets, t and tW channel single top-quark productions, and the WW process are simulated using POWHEG v2 [15–17]. The single top-quark production via s channel, and the WZ process are simulated with MC@NLO [18]. Single boson production (W+jets and Z+jets) is simulated with MADGRAPH v5 [19]. PYTHIA 8.212 [20, 21] is used for the parton shower development and hadronization, and is also used to simulate QCD multijet events.

The cross sections used to normalize the SM processes are calculated to the next-to-leading order (NLO) or the next-to-next-to-leading order (NNLO), when the latter is available [22–24]. For the signal, the NLO cross sections are taken from Ref. [25, 26].

All generated events are processed through the CMS detector simulation based on GEANT4 [27]. Additional minimum-bias events, generated with PYTHIA, are superimposed on the hard-scattering events to simulate multiple pp interactions (pileup) within the same beam crossing as well as in the beam crossings just before and after. The MC events are weighted to reproduce the distribution of the number of pileup interactions in the data.

3 Event reconstruction

All physics objects in the event are reconstructed using a particle-flow (PF) algorithm [28–30], which uses information from all subsystems to reconstruct photons, electrons, muons, charged hadrons and neutral hadrons. The vertex with the highest sum of squared p_T of all associated tracks is taken as the primary vertex of the hard collision. Event cleaning filters are applied to reject events where electronic noise or proton-beam backgrounds mimic energy deposits in the detector.

Electron candidates are reconstructed by combining tracking information with energy deposits in the ECAL in the pseudorapidity range $|\eta| < 2.5$ (excluding the range $1.4442 < |\eta| < 1.566$, which is a gap between endcap and barrel calorimeters). Tight identification criteria are applied to select well-reconstructed electron candidates. Candidates are identified [31] using information on the shower-shape, the track quality and the spatial match between the track and the electromagnetic cluster, the fraction of total cluster energy in the hadronic calorimeter, and the resulting level of activity in the surrounding tracker and calorimeter regions. The momentum resolution for electrons with $p_T > 40$ GeV measured using $Z \to ee$ decays is 1.7% [31] in the central region of the detector.

Muon candidates are identified by reconstruction algorithms using hits in the silicon tracking system and signals in the muon system. To identify the muon candidates, tracks associated to muon candidates must be consistent with a muon originating from the primary vertex and satisfy a set of identification requirements. The matching of muons to tracks in the silicon

tracker results in relative transverse momentum resolution of 1.3-2.0% in the central region of the detector for muons with $20 < p_{\mathrm{T}} < 100$ GeV, and is better than 10% for muons with p_{T} up to 1 TeV [32].

Lepton reconstruction and trigger efficiencies are evaluated in bins of p_{T} and $|\eta|$ in both data and simulation, using a tag-and-probe method [33].

An isolation variable is employed to suppress leptons originating from QCD processes. It is calculated from the transverse energy $E_{T,\mathrm{cone}}$ of particle tracks and deposits in the calorimeter within a cone $\Delta R = \sqrt{(\Delta\eta)^2 + (\Delta\phi)^2} = 0.3(0.4)$ around the trajectory of the electron(muon), where ϕ is the azimuthal angle.

Particles reconstructed by the PF algorithm are clustered into jets by using each particle direction at the interaction vertex. Charged hadrons found by the PF algorithm that are associated with pileup vertices are not considered. Particles that are identified as isolated leptons are removed from the jet clustering procedure. Jets are reconstructed with the anti-kT algorithm [34, 35] with distance R=0.4. An event-by-event jet-area-based correction [36–38] is applied to remove, on a statistical basis, pileup contributions that are not already removed by the described above charged-hadron subtraction procedure. Jet energy corrections are applied to each jet, as a function of $\mathrm{p_T}$ and η, to correct for non-linear effects [36].

The missing transverse energy, $E_{\mathrm{T}}^{\mathrm{miss}}$, is defined as the magnitude of the negative vector sum of the transverse momenta of all the particles found by the PF algorithm. A decay of a heavy quark into a W boson and a b quark is expected to exhibit genuine missing transverse energy because of the undetected neutrino from the leptonically decaying W. A missing transverse energy cut is applied to the selected events, and the missing transverse momentum vector is used in the mass reconstruction.

To identify jets as originating from a b quark (b-tagged jets) the Combined Secondary Vertex (CSV) algorithm was used [39]. This tagging algorithm combines variables which can distinguish b from non-b jets, such as information on track impact parameter significance and secondary vertex properties. The variables are combined using a likelihood ratio technique to compute a b-tag discriminator. We use the medium operating point [39], which achieves a high b-tagging efficiency of approximately 70% and a low mis-tag rate of 1%. Data-to-MC b-tagging efficiency scale factors and mistag rate scale factors account for the small differences between data and MC efficiencies. We use these scale factors as a function of jet p_{T} and η [39].

4 Event selection and search strategy

The event selection requires exactly one lepton (electron or muon) with $p_T > 40$ GeV and $|\eta| < 2.1$. Events with additional leptons passing relatively loose isolation and identification requirements with $p_T > 10$ GeV and $|\eta| < 2.5$ GeV are rejected.

Events are required to have at least two jets, one in the central and one in the forward region of the detector. The central jet is required to have $p_T > 200$ GeV and $|\eta| < 2.4$ and be b-tagged. In case of more than one central jet present, the jet with the largest p_T is further employed in reconstructing the mass of the VLQ. The forward jet ($2.4 < |\eta| < 5.0$) must have $p_T > 30$ GeV.

In the single VLQ production, the b quark and the W boson tend to be in opposite directions. Hence, the azimuthal angle between the central b-jet and the lepton is required to satisfy $\Delta\phi(\ell, \mathrm{b}) > 2$. In addition, the lepton is required to be separated from any jets produced in the event. In case there is a jet within $\Delta R(\ell, \mathrm{jet}) < 1.5$, such an event is rejected. Since W bosons

originating from heavy VLQ decay are produced with significant boost, events are required to have substantial missing transverse energy $E_{\mathrm{T}}^{\mathrm{miss}} > 50$ GeV due to undetected neutrino from W decay. The transverse mass formed by the lepton and $E_{\mathrm{T}}^{\mathrm{miss}}$ system is required to satisfy $M_T < 130$ GeV to suppress $\mathrm{t\bar{t}}$ dilepton events, which can mimic our signal when one of the leptons escapes detection.

Finally, events are required to have $\mathrm{S_T} > 500$ GeV, where $\mathrm{S_T}$ is defined as the scalar sum of the transverse momenta of the lepton, the leading central jet and missing transverse energy : $\mathrm{S_T} = \mathrm{p_T^{\ell}} + \mathrm{p_T^{\text{leading jet}}} + \mathrm{E_T^{miss}}$.

The mass of the heavy quark candidate is reconstructed as an invariant mass M_{inv} of its decay products: the lepton, the leading central jet and the neutrino, where the x,y-components of the neutrino momentum are given by the missing transverse momentum, while the z-component is determined by constraining the invariant mass of the lepton and neutrino four-momenta to the W boson mass value.

New physics arising from the single VLQ production $\mathrm{Y/T} \to \mathrm{Wb}$ would result in a peak in the M_{inv} distribution. The search is thus performed by fitting the observed M_{inv} distribution to a combination of SM background processes plus new physics signal.

5 Background modeling

The dominant backgrounds in this search are $\mathrm{t\bar{t}}$ and W + jets events. The modeling of these processes is validated by studying dedicated background-enriched samples.

For the $\mathrm{t\bar{t}}$ process, we select events with a single lepton with $p_T > 40$ GeV and $|\eta| < 2.1$, $E_T^{miss} > 50$ GeV, and at least 2 b-tagged jets with the leading(sub-leading) jet $p_T > 70$ (30) GeV. The top p_T spectrum in the $\mathrm{t\bar{t}}$ simulation is known to be mis-modeled and it is reweighted using the empirical function in Ref. [40]. After this correction, a good agreement is observed for all relevant kinematic variables. S_T and M_{inv} distributions are shown in Figure 2.

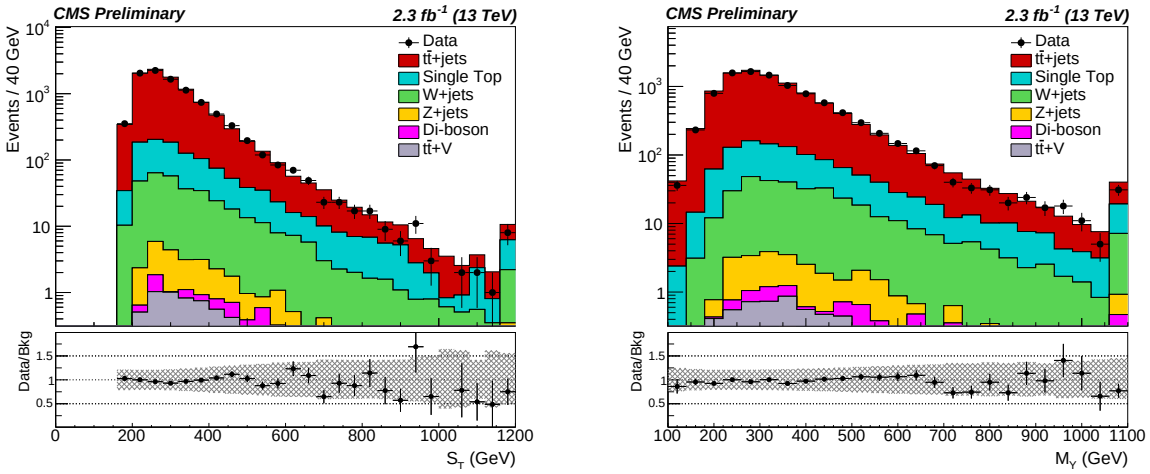

(a) S_T distribution

(b) M_{inv} distribution

Figure 2: Kinematic distributions in the $\mathrm{t\bar{t}}$-enriched control sample

The W + jets enriched control sample consists of events with a single lepton with $p_T > 40$ GeV and $|\eta| < 2.1$, $E_T^{miss} > 50$ GeV, leading jet with $p_T > 200$ GeV and $|\eta| < 2.4$, and at least

one forward jet with $p_T > 30$ GeV and $|\eta| > 2.4$. The lepton is required to be in the opposite direction ($\Delta\phi(\ell, \text{jet}) > 2$) from the leading jet and no jets should be present with $\Delta R(\ell, \text{jet}) < 1.5$. This control region resembles the signal selection except that events with b-tagged jets are vetoed.

We observe that in the W+jets simulated sample the number of events in the tails of the jet p_T distributions are overestimated compared to the measured distributions in data. We derive the correction to the W+jets simulation using the H_T variable, which is defined as the sum of the transverse momenta of all jets with $p_T > 40$ GeV. The data to simulation ratio of the H_T distribution is well described by a 2-parameter linear fit with a negative slope. A correction to the modeling of the W+jets H_T spectrum is made using the results of the fit. After the correction, a good agreement in the modeling of all kinematic variables is observed. Distributions of S_T and invariant mass of the Wb system are shown in Figure 3.

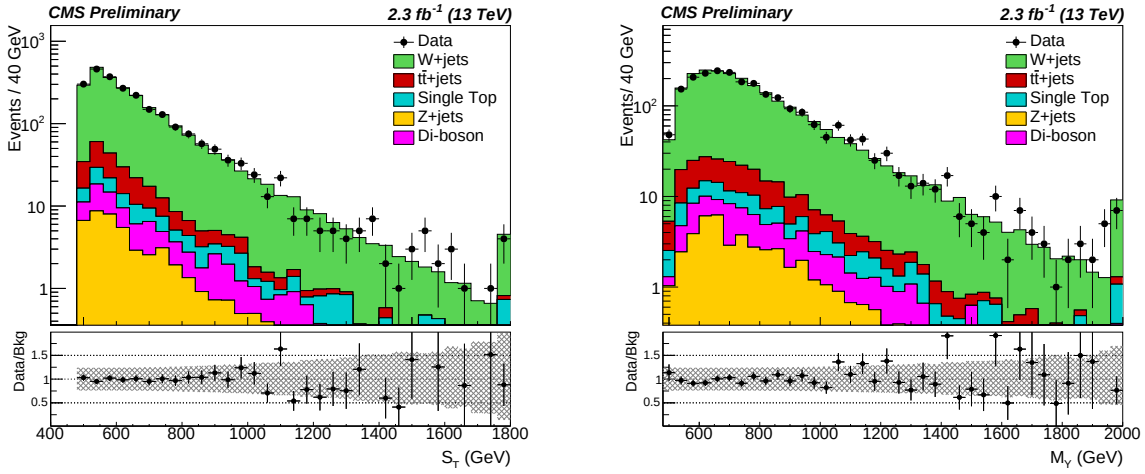

(a) S_T distribution (b) M_{inv} distribution

Figure 3: Kinematic distributions in the W+jets-enriched control sample

6 Systematic uncertainties

Systematic uncertainties can be divided into two categories: uncertainties that impact only the rate of background and signal predictions, and uncertainties that affect the shape of the fitted M_{inv} spectra.

Shape uncertainties of the M_{inv} distribution are modeled by varying the nuisance parameter that characterizes the respective systematic effect up and down by one standard deviation.

The uncertainty on the integrated luminosity is 2.7%. We assign the uncertainties for normalization of the SM background processes based on corresponding CMS cross section measurements at 13 TeV, which are 5.6% for $\text{t}\bar{\text{t}}$ [41], 14.7% for single top [42], and 9.2% for W+jets [43], where in the latter we also account for uncertainties in the W+heavy flavor contributions [44, 45].

To account for $\text{t}\bar{\text{t}}$ and W+jets kinematics mis-modeling in simulation we assign uncertainties arising from the top p_T re-weighting procedure and from the H_T correction, respectively. In both cases, the uncertainty is assigned as a band, with one side obtained without the reweighting or correction procedure, and with the other side obtained by applying the procedure twice.

In addition, the reconstruction efficiency of forward jets has been observed to be larger in the simulation as compared to the data. The efficiency as a function of η is corrected to match the data using the W+jets-enriched sample with 0 b-tag events, and validated using the $t\bar{t}$-enriched sample of events with 2 b-tags. A rate uncertainty of $\pm$ 15% is assigned to the forward jet modeling in simulation.

Trigger and lepton identification efficiencies in simulation are corrected as a function of lepton p_T and η using decays of Z bosons to dileptons in data. The associated uncertainty of about 2% is derived based on available statistics.

Shape uncertainties include uncertainties on the jet energy scale, jet energy resolution, b-tagging efficiency, pileup, parton distribution functions (PDF), as well as factorization and renormalization scales affecting the determination of the strong coupling constant $\alpha_s(Q^2)$.

The uncertainty related to the modeling of pileup is evaluated by varying the minimum bias cross-section by $\pm$5% relative to the nominal value of 69 mb. Uncertainties due to renormalization and factorization scales are taken into account by varying both scales simultaneously up and down by a factor of two. Uncertainties arising from the choice of PDFs are taken into account by weighting simulated events according to the uncertainties parametrized by the CTEQ6 eigenvectors [46].

Systematic uncertainties are summarized in Table 1.

Table 1: Summary of the systematic uncertainties for the background MC and signal samples.

source		W+Jets	$t\bar{t}$	Single Top	Signal
Luminosity	rate	2.7%	2.7 %	2.7 %	2.7 %
Jet energy scale	shape	5%	6%	5%	3%
Jet energy resolution	shape	2%	1%	1%	2%
B-tagging efficiency	shape	3%	5%	5%	5%
Multiple interactions	shape	1%	1%	1%	1%
Lepton ID/ISO scale factor	rate	2%	2%	2%	2%
Trigger efficiency	rate	2%	2%	2%	2%
Cross Section	rate	9.2%	5.6%	14.7%	–
Top P_T reweighting	shape	–	38%	–	–
W+jets H_T reweighting	shape	5.3%	–	–	–
Q^2 Scale	shape	14%	16%	16%	25%
PDF	shape	5.5%	2.3%	8.5%	6.7%
Forward jet reweighting	rate	15%	15%	15%	15%

7 Limit calculation and results

A good agreement between the data and SM predictions is observed, as shown in Table 2. The M_{inv} spectrum is fitted to a combination of SM backgrounds processes plus new physics signal.

In the likelihood fit contributions from the SM processes are allowed to float independently within their normalization systematic uncertainties, using log-normal priors. The nuisance parameters describing the shape uncertainties, are constrained using gaussian priors. The shapes of the M_{inv} distributions for backgrounds and signal are parametrized and varied according to the nuisance parameters. The post-fit M_{inv} distribution, with the shape and background normalizations corresponding to the maximum likelihood values, is presented in Figure 4.

No evidence for an excess over the SM background expectations is observed. The 95% C.L. upper limits on the production cross section of $Y/T \rightarrow Wb$ process are computed using a Bayesian

interpretation, where the likelihood is marginalized with respect to the nuisance parameters representing systematic uncertainties. For interpretation of results for Y quark production, we set the coupling to the W boson and the b quark to 0.5 and the BR(Y→Wb)=100%. For T quark production corresponding values are 1 for the coupling and 50% for the BR(T→Wb). The 95% C.L. expected and observed upper limits are listed in Table 3. Figures 5, 6 and 7 show the exclusion limits in the two-dimensional space of the mass of the heavy quark and its electroweak coupling c^{bW}.

Table 2: Data, background and signal (m(Y) = 1000 GeV mass point with the NLO cross section [26]) pre-fit event yields corresponding to 2.3 fb^{-1} of integrated luminosity. Percentage numbers in the signal column indicates the signal acceptance efficiency. The error on the backgrounds includes both pre-fit statistical and systematic uncertainties.

Channel	W+jets	$t\bar{t}$	Single Top	QCD	Z+jets	Di-boson	Y(1000)	Total bkg	Data
Electron	$44.5^{+11.4}_{-12.4}$	$28.1^{+11.7}_{-10.2}$	$19.9^{+4.7}_{-4.9}$	$0.0^{+1.0}_{-0.0}$	$1.5^{+1.5}_{0.0}$	$1.3^{+0.5}_{-0.5}$	54.1(1.3%)	$95.3^{+30.8}_{-27.9}$	78
Muon	$52.4^{+13.2}_{-14.4}$	$33.8^{+13.7}_{-12.0}$	$26.6^{+6.2}_{-6.3}$	$0.0^{+1.0}_{-0.0}$	$0.7^{+0.7}_{0.0}$	$1.7^{+0.6}_{-0.6}$	60.2(1.4%)	$115.2^{+34.9}_{-33.3}$	95

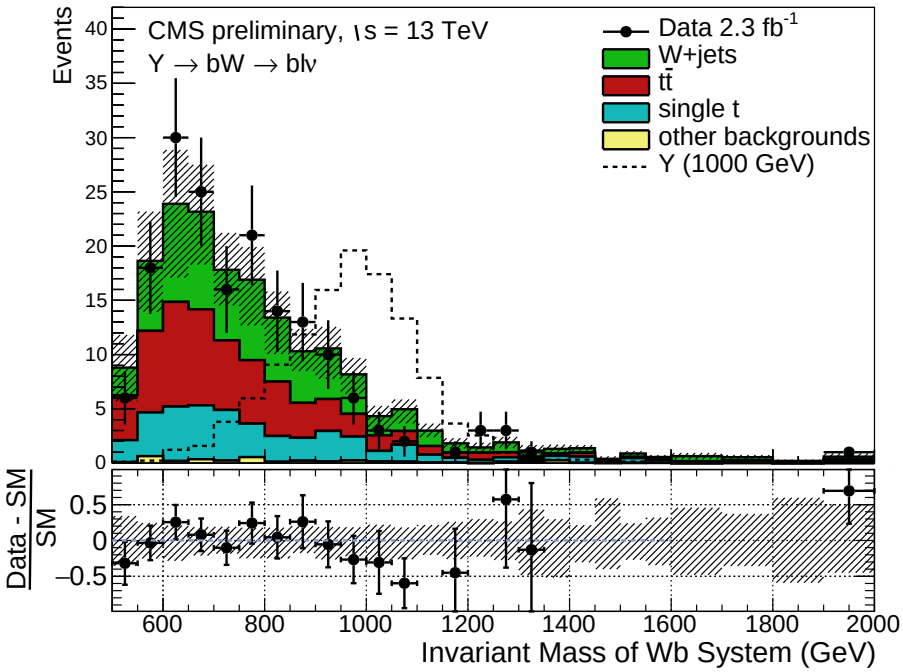

Figure 4: The invariant mass M_{inv} distribution after the fit. In the last bin the data overflow event is an electron channel event with a mass of 2215 GeV.

8 Summary

The results for the single production of the vector-like quark decaying exclusively into a W boson and a b quark are presented. The search is performed in the electron/muon + jets channels. The mass of the vector-like quark is reconstructed by forming the invariant mass of the leading b-jet, electron or muon and reconstructed neutrino in the event, and the fit to the invariant mass spectrum is performed. No evidence of an excess due to new physics is observed, and 95% C.L. upper limits are set on the single vector-like production cross section in the mass range from 700 to 1800 GeV. The results are also interpreted as limits on the mass of the vector-like quark

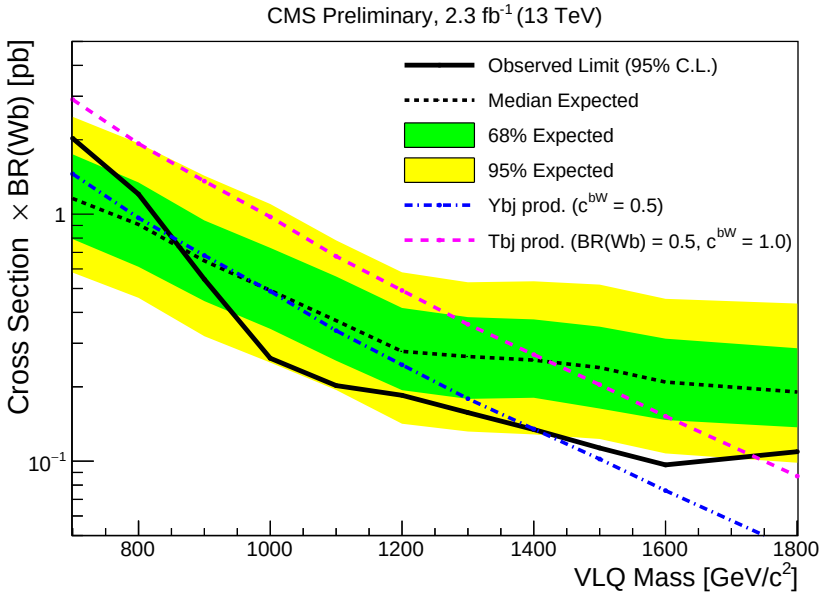

Figure 5: Expected and observed limits on the single VLQ production cross section together with the 1- and 2- sigma uncertainty bands.

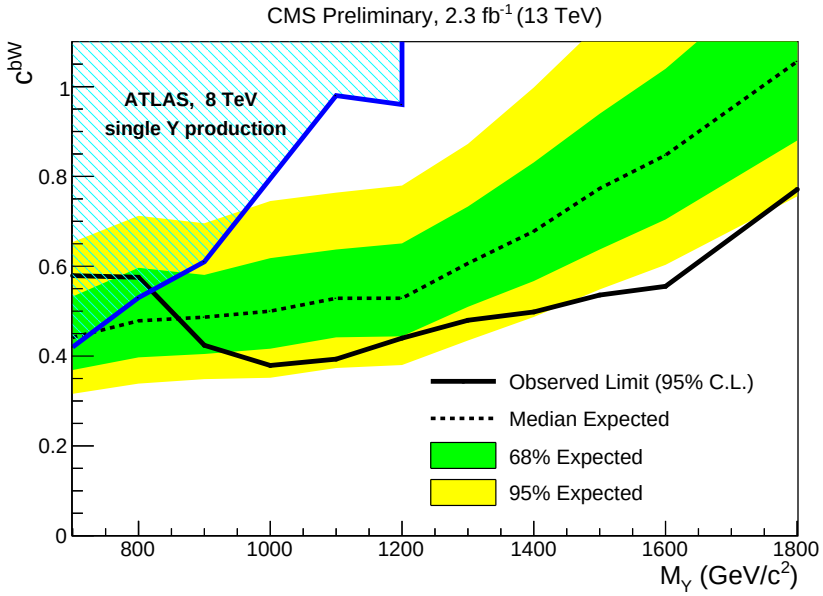

Figure 6: Expected and observed limits on the electroweak coupling of the Y quark as a function of its mass. The region above the observed limit is excluded in this analysis at 95% C.L.

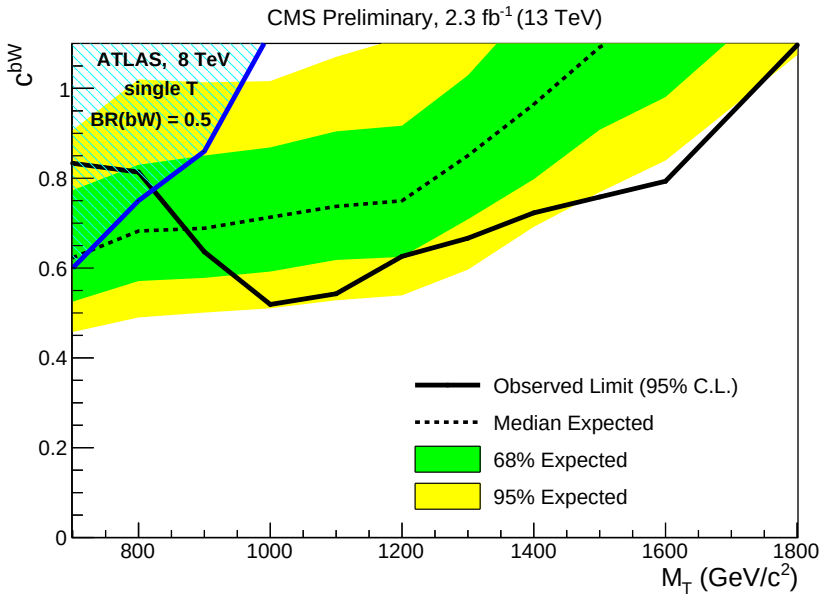

Figure 7: Expected and observed limits on the electroweak coupling of the T quark as a function of its mass. The region above the observed limit is excluded in this analysis at 95% C.L.

Table 3: Expected and observed upper limits on the single VLQ production cross section ($\sigma\times$ BR(Q$\rightarrow$Wb)=100%)

VLQ mass (GeV)	Expected UL (pb)	Observed UL (pb)
M(700)	1.16	2.03
M(800)	0.91	1.20
M(900)	0.65	0.54
M(1000)	0.49	0.26
M(1100)	0.37	0.20
M(1200)	0.28	0.18
M(1300)	0.27	0.16
M(1400)	0.26	0.13
M(1500)	0.24	0.11
M(1600)	0.21	0.10
M(1700)	0.20	0.10
M(1800)	0.19	0.11

and its coupling to the W boson and the b quark. T quarks with masses below 1.73 TeV are excluded at 95% C.L. assuming a unit coupling and a BR(T$\rightarrow$Wb) = 0.5, while the expected limit is 1.42 TeV. Y quarks with coupling of 0.5 and a BR(Y$\rightarrow$Wb) = 1 are excluded below 1.40 TeV, whereas the expected limit is 0.99 TeV.

References

[1] ATLAS Collaboration, "Observation of a new particle in the search for the Standard Model Higgs boson with the ATLAS detector at the LHC", *Phys. Lett. B* **716** (2012) 1, doi:10.1016/j.physletb.2012.08.020, arXiv:1207.7214.

[2] CMS Collaboration, "Observation of a new boson at a mass of 125 GeV with the CMS experiment at the LHC", *Phys. Lett. B* **716** (2012) 30, doi:10.1016/j.physletb.2012.08.021, arXiv:1207.7235.

[3] P. Lodone, "Vector-like quarks in a 'composite' Higgs model", *JHEP* **0812** (2008) 029, doi:10.1088/1126-6708/2008/12/029, arXiv:0806.1472.

[4] M. Perelstein, M. E. Peskin, and A. Pierce, "Top quarks and electroweak symmetry breaking in little Higgs models", *Phys.Rev.* **D69** (2004) 075002, doi:10.1103/PhysRevD.69.075002, arXiv:hep-ph/0310039.

[5] R. Contino, T. Kramer, M. Son, and R. Sundrum, "Warped/composite phenomenology simplified", *JHEP* **0705** (2007) 074, doi:10.1088/1126-6708/2007/05/074, arXiv:hep-ph/0612180.

[6] CMS Collaboration, "Search for vectorlike charge 2/3 T quarks in proton-proton collisions at $\sqrt{s}$ = 8 TeV", *Phys. Rev. D* **93** (2016) 012003, doi:10.1103/PhysRevD.93.012003, arXiv:1509.04177.

[7] CMS Collaboration, "Search for pair-produced vector-like B quarks in proton-proton collisions at $\sqrt{s}$ = 8 TeV", *Phys. Rev. D* **93** (2016) 112009, doi:10.1103/PhysRevD.93.012003, arXiv:1507.07129.

[8] ATLAS Collaboration, "Search for production of vector-like quark pairs and of four top quarks in the lepton-plus-jets final state in pp collisions at $\sqrt{s}$ = 8 TeV with the ATLAS detector", *J. of High Energy Phys.* **08** (2015) 105, doi:10.1007/JHEP08(2015)105, arXiv:1505.04306.

[9] ATLAS Collaboration, "Search for vector-like B quarks in events with one isolated lepton, missing transverse momentum and jets at $\sqrt{s}$ = 8 TeV with the ATLAS detector", *Phys. Rev. D* **91** (2015) 112011, doi:10.1103/PhysRevD.91.112011, arXiv:1503.05425.

[10] J. A. Aguilar-Saavedra, R. Benbrik, S. Heinemeyer, and M. Perez-Victoria, "A handbook of vector-like quarks: mixing and single production", *Phys. Rev. D* **88** (2013) 094010, doi:10.1103/PhysRevD.88.094010, arXiv:arXiv:1306.0572.

[11] CMS Collaboration, "Search for Single Production of a Vector Like T Quark Decaying to a Higgs Boson and a Leptonically Decaying Top Quark", CMS Physics Analysis Summary CMS-PAS-B2G-15-008, 2016.

[12] CMS Collaboration, "Search for single production of vector-like quarks decaying into final states with a Z boson and a top or a bottom quark", CMS Physics Analysis Summary CMS-PAS-B2G-16-001, 2016.

[13] ATLAS Collaboration, "Search for single production of vector-like quarks decaying into Wb in pp collisions at $\sqrt{s} = 8$ with the ATLAS detector", *Submitted to Eur. Phys. J. C* (2016) arXiv:1602.05606v1.

[14] CMS Collaboration, "The CMS experiment at the CERN LHC", *JINST* **3** (2008) S08004, doi:10.1088/1748-0221/3/08/S08004.

[15] P. Nason, "A new method for combining NLO QCD with shower Monte Carlo algorithms", *JHEP* **11** (2004) 040, doi:10.1088/1126-6708/2004/11/040, arXiv:hep-ph/0409146.

[16] S. Frixione, P. Nason, and C. Oleari, "Matching NLO QCD computations with parton shower simulations: the POWHEG method", *JHEP* **11** (2007) 070, doi:10.1088/1126-6708/2007/11/070, arXiv:0709.2092.

[17] S. Alioli et al., "A general framework for implementing NLO calculations in shower Monte Carlo programs: the POWHEG BOX", *JHEP* **06** (2010) 043, doi:10.1007/JHEP06(2010)043, arXiv:1002.2581.

[18] J. Alwall et al., "The automated computation of tree-level and next-to-leading order differential cross sections, and their matching to parton shower simulations", *JHEP* **07** (2014) 079, doi:10.1007/JHEP07(2014)079, arXiv:1405.0301.

[19] J. Alwall et al., "MadGraph 5: Going Beyond", *JHEP* **06** (2011) 128, doi:10.1007/JHEP06(2011)128, arXiv:1106.0522.

[20] T. Sjöstrand, S. Mrenna, and P. Z. Skands, "PYTHIA 6.4 physics and manual", *JHEP* **05** (2006) 026, doi:10.1088/1126-6708/2006/05/026, arXiv:0603175.

[21] T. Sjöstrand, S. Mrenna, and P. Z. Skands, "An Introduction to PYTHIA 8.2", *Comput. Phys. Comm* **191** (2015) 159–177, doi:10.1016/j.cpc.2015.01.024, arXiv:1410.3012.

[22] a. a. T. Gehrmann, "W^+W^- production at hadron colliders in NNLO QCD", *Phys. Rev. Lett.* **113** (2014) 212001, doi:10.1103/PhysRevD.88.094010, arXiv:http://arxiv.org/abs/1408.5243.

[23] M. Czakon and A. Mitov, "NNLO corrections to top pair production at hadron colliders: the quark-gluon reaction", *JHEP* **01** (2013) 080, doi:doi:10.1007/JHEP01(2013)080.

[24] N. Kidonakis, "Next-to-next-to-leading-order collinear and soft gluon corrections for t-channel single top quark production", *Phys. Rev. D* **83** (2011) 091503, doi:http://journals.aps.org/prd/abstract/10.1103/PhysRevD.83.091503, arXiv:http://arxiv.org/abs/1103.2792.

[25] R. K. E. John Campbell and F. Tramontano, "Single top production and decay at next-to-leading order", *Phys. Rev.* **70** (2004) 094012, doi:10.1103/PhysRevD.70.094012, arXiv:arXiv:hep-ph/0408158.

[26] O. M. Giuliano Panico and A. Wulzer, "On the Interpretation of Top Partners Searches", *JHEP* **12** (2014) 097, doi:10.1007/JHEP12(2014)097, arXiv:arXiv:1409.0100.

[27] GEANT4 Collaboration, "GEANT4 – a simulation toolkit", *Nucl. Instrum. Meth. A* **506** (2003) 250, doi:10.1016/S0168-9002(03)01368-8.

[28] CMS Collaboration, "Particle-Flow Event Reconstruction in CMS and Performance for Jets, Taus, and MET", CMS Physics Analysis Summary CMS-PAS-PFT-09-001, 2009.

[29] CMS Collaboration, "Commissioning of the Particle-Flow Reconstruction in Minimum-Bias and Jet Events from pp Collisions at 7 TeV", CMS Physics Analysis Summary CMS-PAS-PFT-10-002, 2010.

[30] CMS Collaboration, "Particle-flow commissioning with muons and electrons from J/Psi and W events at 7 TeV", CMS Physics Analysis Summary CMS-PAS-PFT-10-003, 2010.

[31] CMS Collaboration, "Performance of Electron Reconstruction and Selection with the CMS Detector in Proton-Proton Collisions at $\sqrt{s}$ = 8 TeV", *JINST* **10** (2015) P06005, doi:doi:10.1088/1748-0221/10/06/P06005, arXiv:1502.02701.

[32] CMS Collaboration, "Description and performance of track and primary-vertex reconstruction with the CMS tracker", *JINST* **9** (2014) P10009, doi:doi:10.1088/1748-0221/9/10/P10009, arXiv:1405.6569.

[33] CMS Collaboration, "Measurements of Inclusive W and Z Cross Sections in pp Collisions at $\sqrt{s}$ = 7 TeV", *JHEP* **01** (2011) 080, doi:10.1007/JHEP01(2011)080.

[34] M. Cacciari and G. P. Salam, "Dispelling the N^3 myth for the k_t jet-finder", *Phys. Lett. B* **641** (2006) 57, doi:10.1016/j.physletb.2006.08.037, arXiv:hep-ph/0512210.

[35] M. Cacciari, G. P. Salam, and G. Soyez, "The anti-k_t jet clustering algorithm", *JHEP* **04** (2008) 063, doi:10.1088/1126-6708/2008/04/063, arXiv:0802.1189.

[36] CMS Collaboration, "Determination of jet energy calibration and transverse momentum resolution in CMS", *JINST* **6** (2011) P11002, doi:10.1088/1748-0221/6/11/P11002, arXiv:1107.4277.

[37] M. Cacciari, G. P. Salam, and G. Soyez, "The catchment area of jets", *JHEP* **04** (2008) 005, doi:10.1088/1126-6708/2008/04/005, arXiv:0802.1188.

[38] M. Cacciari and G. P. Salam, "Pileup subtraction using jet areas", *Phys. Lett. B* **659** (2008) 119, doi:10.1016/j.physletb.2007.09.077, arXiv:0707.1378.

[39] CMS Collaboration, "Performance of b tagging at $\sqrt{s}$=8 TeV in multijet, $t\bar{t}$ and boosted topology events", CMS Physics Analysis Summary CMS-PAS-BTV-13-001, 2013.

[40] CMS Collaboration, "Measurement of the differential cross section for top quark pair production in pp collisions at $\sqrt{s}$ = 8 TeV", *Eur. Phys. J. C* **75** (2015) 542, doi:10.1140/epjc/s10052-015-3709-x, arXiv:1505.04480.

[41] CMS Collaboration, "Measurement of the $\mathrm{t\bar{t}}$ production cross section in the dilepton channel in pp collisions at $\sqrt{s}$ = 8 TeV", *JHEP* **02** (2014) 024, doi:10.1007/JHEP02(2014)024, arXiv:1312.7582.

[42] CMS Collaboration, "Measurement of the inclusive cross section of single top-quark production in the t-channel at 13 TeV", CMS Physics Analysis Summary CMS-PAS-TOP-16-003, 2016.

[43] CMS Collaboration, "Measurement of inclusive W and Z boson production cross sections in pp collisions at $\sqrt{s}$=13 TeV", CMS Physics Analysis Summary CMS-PAS-SMP-15-004, 2015.

[44] CMS Collaboration, "Measurement of associated W + charm production in pp collisions at $\sqrt{s}$ = 7 TeV", CMS Physics Analysis Summary CMS-SMP-12-002, 2013.

[45] CMS Collaboration, "Measurement of the W boson production cross section in association with two b jets in pp collisions at $\sqrt{s}$=8 TeV", CMS Physics Analysis Summary CMS-PAS-SMP-14-020, 2014.

[46] J. Pumplin et al., "New generation of parton distributions with uncertainties from global QCD analysis", *J. High Energy Phys.* **07** (2002) 012.